Three-dimensional unified theoretical approach to ultimate horizontal pullout capacity of vertical square anchor

Wei Hu[1,2], Y. Chen[1,2], W.-H. Gao[1,2], L. Yong[1,2], C.-F. Zeng[1,2], Y.-X. Pen[1,2]

[1] Hunan Province Key Laboratory of Geotechnical Engineering Stability Control and Health Monitoring, Hunan University of Science and Technology, Xiangtan 411201, China.
[2] School of Civil Engineering, Hunan University of Science and Technology, Xiangtan 411201, China.

ABSTRACT

Horizontal pullout mechanism and bearing capacity research of vertical square anchor plate has the problem of artificial distinguishing shallow and deep buried types, but non-uniform definition standard. The presented thesis is devoted to the research of three-dimensional unified model and theoretical approach of horizontal ultimate pullout capacity of vertical square anchor plate based on deep analysis of failure mechanism. Symmetry of failure mechanism varying with soil property and buried depth ratio in vertical and horizontal directions were reflected by the evolution of projected triangles of rectangular pyramid soil core before anchor plate to the vertical plane and horizontal plane respectively under ultimate load. Based on that, Three-dimensional unified mechanical model was built and corresponding theoretical approach was derived using limit equilibrium analysis method. Comparison with test datum indicated that new approach performed the best for the calculation was more closely to the measured values with smaller discreteness and the average was generally safe compared with three other methods.

Keywords: vertical square anchor; horizontal pullout capacity; mechanical model; three-dimensional unified theoretical approach

1 INTRODUCTION

In the design of anchor plate retaining wall, the ultimate horizontal pulling capacity of vertical anchor plate must be determined. However, the current research on the bearing capacity of vertical anchor plate mainly focuses on strip anchor plate(G.S. Kame et al., 2012), while rectangular or circular anchor plate considers its three-dimensional effect by introducing the method of shape coefficient on this basis(Zhu et al., 2006), and there is almost no research on the direct three-dimensional theoretical analysis.In addition, the current research generally follows the definition of shallow or deep buried first, and then, using the assumption of fixed asymmetric or symmetric form of sliding line field to construct mechanical models for shallow and deep buried anchor plate respectively(Miyata, Y. et al., 2011; Neely, W.J. et al., 1972). However, the symmetry of slip line field should not be fixed artificially, nor should there be a fixed boundary between shallow buried and deep buried. Based on vertical square anchor plate as the object, the research aims to build the three-dimensional mechanical model under ultimate horizontal pulling which can reflect the symmetry properties of slip line field in front of the plate varying with buried depth ratio and soil parameters continuously, without artificial distinguishing shallow anchor from a deep anchor. Unified theoretical approach of the ultimate bearing capacity will be derived based on limit equilibrium analysis, whose rationality will be validated by comparing with three other theoretical methods , laboratory and field test results.

2 MODEL AND THEORETICAL DERIVATION

Under horizontal pulling load, a four-pyramid soil core will be formed gradually in front of the squre plate, whose force diagram is shown in Figure 1.

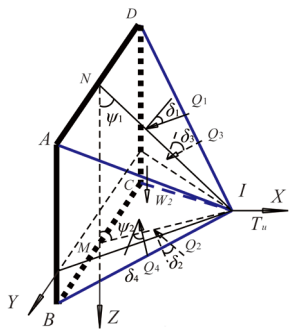

Fig.1. Rectangular pyramid soil core before plate

The resultant soil pressures on the four sides of the core are Q_1, Q_2, Q_3 and Q_4 respectively, and the angles between these forces to the normal directions of the corresponding surfaces are δ_1, δ_2, δ_3 and δ_4. Two base angles of triangle MNI, ψ_1 and ψ_2 satisfy the Eq. (1).

$$\begin{aligned} &\varphi \le \psi_1 \le \pi/4 + \varphi/2 \\ &\pi/2 \ge \psi_2 \ge \pi/4 + \varphi/2 \\ &\psi_1 + \psi_2 = \pi/2 + \varphi \end{aligned} \tag{1}$$

φ is the internal friction angle of soil. After the rectangular pyramid soil core formed, the four sides will continue to extrude the soil in the direction they faced in the subsequent pulling process, and eventually form a three-dimensional sliding body in front of the plate as shown in figure 2 when the pulling enters into failure state.

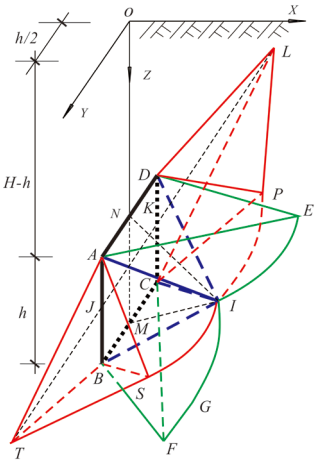

Fig.2. Three-dimensional sliding body before plate

The green sliding body is formed by the vertical (Z direction) compression of the upper and lower sides of the soil core.The red sliding body is formed by the horizontal (Y direction) compression of the front and back sides of the soil core. ∠FMN changes with the increase of buried depth ratio from π/2 to (π/4+φ/2)+π/2, ∠FMI satisfies the Eq. (2).

$$\angle FMI = -\pi(2\psi_2 - \pi)/(\pi - 2\varphi) \tag{2}$$

The triangular body ADEI, the curved edge body BCFGI, ABTGI and CDLPI were taken in turn for mechanical equilibrium analysis, and the resultant soil pressures on the four sides of rectangular pyramid soil core were obtained as Eq. (3) to Eq. (5).

$$Q_1 = \frac{(W_1 + qs_{\Delta ADE})\sin(\alpha+\beta)}{\sin(\pi/2 + \psi_1 - \delta_1 - \alpha - \beta)} \tag{3}$$

$$Q_2 = \sqrt{T_1^2 + [R_3(R_5)]^2 - 2T_1[R_4(R_6)]}\cos(\theta_1 - \angle 1) \tag{4}$$

$$Q_3 = Q_4 = q_u S \tag{5}$$

W_1 is the weight of triangular body ADEI; α=π/4-φ/2; $R_1(R_2)$ is the sum of the vertical components of the soil pressure resultant forces on surface DEI and surface AEI; β is the angle between $R_1(R_2)$ and line EI; δ_1=arctan(c/σ+tanφ); c is the conhesion parameter of soil; σ is the average soil pressure on △ADI; $q_1$is the uniformly distributed load equivalent to the weight of soil above △ADE, which is equal to $\gamma(H-h)$; $R_3(R_5)$ represents the sum of vertical components of the earth pressure resultant force R_3 on surface CGI and R_5 on △BGI, while $R_4(R_6)$ represents the sum of vertical components of the earth pressure resultant force R_4 on surface BFG and R_6 on △CFG; T_1 is the resultant force of resultant soil pressure acted on △BCF, $R_4(R_6)$ and gravity of curved edge BCFGI; ∠1 is the angle between T_1 and $R_4(R_6)$ while θ_1 is the ones of $R_3(R_5)$ to $R_4(R_6)$; areas of △ABI and △CDI are equal to S; $q_u=q_2N_q+cN_c$, q_2 is the arverage earth pressure at rest acted on △ABT and △CDL; N_q and N_c are coefficients of Meyerhof foundation ultimate bearing capacity; the angle between surface ABI to plate is ζ, so is the angle between surface CDI to plate.

Taking soil core of ABCDI as the research object, the vertical mechanical equilibrium equation is shown in Eq. (6).

$$Q_1\sin(\psi_1 - \delta_1) + W_2 - Q_2\sin(\psi_2 - \delta_2) = 0 \tag{6}$$

W_2 is the soil weight of pyramid ABCDI. ψ_1 can be solved by the above equation, and then Q_1, Q_2 can be calculated by Eq. (3) and Eq. (4).

The formula for calculating the ultimate bearing capacity of square anchor plate in horizontal pulling can be obtained from the mechanical equilibrium relation in horizontal direction as shown in Eq. (7).

$$\begin{aligned} T_u = {} & Q_1\cos(\psi_1 - \delta_1) + Q_2\cos(\psi_2 - \delta_2) \\ & + Q_3\cos(\zeta - \delta_3) + Q_4\cos(\zeta - \delta_4) \end{aligned} \tag{7}$$

3 VERIFICATION

For a square anchor plate with a size of 0.3 m in the soil with weight γ=15kN/m^3, same internal friction angle φ and different cohesion c, Figure 3 shows the regulation of upper and lower base angles of the soil core, Ψ_1, Ψ_2 and their ratios versus the buried depth H/h. It can be seen that, with different cohesion c, as the depth ratio increases, the upper base angle Ψ_1 increases while the lower base angle Ψ_2 decreases, and Ψ_2/Ψ_1 approaches to 1 , which is in good agreement with the expectation of the model. It means that the model can unified express the characteristics of shallow buried and deep buried anchor plates effectively.

32 data points of field and indoor large-size pulling test on square anchor plate as shown in Table 1, these datas were collected from China, Japan and the United States. Three other methods of PWRC, Miyata amendment and Terzaghi will be used to calculate the ultimate bearing capacity of anchor plates in Table 1, and then compare with the results of three-dimentional

Table 1 Summary of site and laboratory anchor-plate pullout tests

Test series	Soil	Tri-axial test type	φ (deg)	c (kPa)	γ (kN/m^3)	Plate size B (m)	Depth (m)	T_u (kN)	References	Place
1	Cohesive soil	CU	29.5	19.6	19.7	0.5	2	333.2		Field test, China
2							4	321.4		
3						0.75	2	364.6		
4							3	153		
5	Cohesive soil	CU	26.5	19.6	16.7	0.5	3	205.8		Field test, China
6							3	235.2		
7						0.75	3	368.5	Zhang et al., 1996	
8							3	431.2		
9	Cohesive soil	CU	29	26.5	18.7	0.6	3	305.8		Field test, China
10	Cohesive soil	CU	26.5	19.6	19.4	0.8	3.3	520.6		Field test, China
11	Cohesive soil	CU	32	8.96	15.7	0.9144	2.286	711.68	J.E. Smith,1957	Field test, USA
12	Sandy soil	CD	35	0	15.1	0.106	3.311	24.8	Takeoka et al., 2009	Laboratory, Japan
13							6.623	34.2		
14							9.934	42.6		
15						0.125	3.311	31.2		
16							6.623	42.2		
17							9.934	56.6		
18	Coarse sand	CD	36	0	16	0.3	2	103	PWRC,1995	Laboratory, Japan
19							3	111.8		
20							4	117.8		
21							5	119.1		
22	Fine sand	CU	30	2	15.4	0.3	2	60.8	Miyata et al., 2010	Laboratory, Japan
23							3	83.8		
24							4	89.4		
25							5	82.4		
26	Silt sand	CU	11	4	15.2	0.3	3	40.6	Miyata et al., 2011	Laboratory, Japan
27							3	44.4		
28							4	44.8		
29							4	50.5		
30	Cohesive soil	CU	13.1	18	15	0.1	0.3	1.847	Fukuoka et al., 1984	Laboratory, Japan
31						0.1	0.5	3.038		
32						0.2	0.5	12.58		

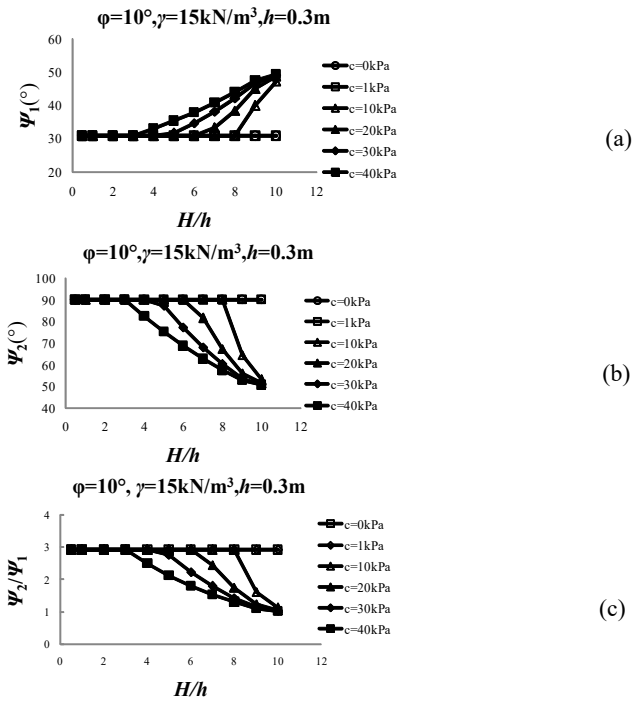

Fig.3. Upper and lower angles versus buried ratio

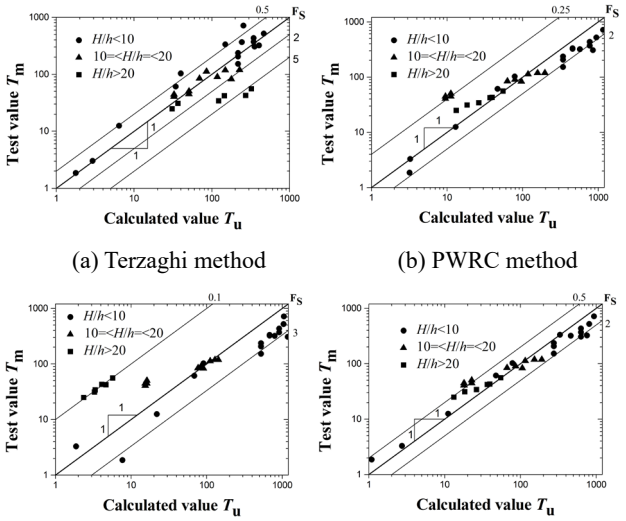

Fig.4. Comparison of different methods

unified theoretical approach proposed in this paper. The comparison results are shown in Figure 4. It can be seen from the figures that under different buried depth ratios,

the ratio(F_s) points of T_u calculated by Terzaghi method to the measured value T_m are evenly distributed on both sides of the 1:1 line, only for the buried depth ratio H/h>20, the calculated value is more serious larger, and the maximum is more than 5 times of the measured one. Compared with the Terzaghi method, F_s of the PWRC method has a more obvious tendency due to the buried depth ratio. When the depth ratio *H/h*<10, the calculation value is general too large. When the buried depth ratio H/h is between 10 and 20, most of them are uniformly located on both sides of the 1:1 line, except for the fact that some individual data points are too small. After the buried depth ratio *H/h*>20, the calculated value is generally small. Miyata proposed an amendment to PWRC method based on a large number of experimental data, but the calculations show that the correction doesn't work very well, which further magnifies the tendency of the PWRC method to be affected by the buried depth ratio. When the buried depth ratio *H/h*<10, the calculation value is general too large, and the maximum is more than 3 times of the measured value, which is dangerous. When the buried depth ratio is *H/h*>20, the calculated value is only 10% of the measured value. The ultimate bearing capacity of the anchor plate is seriously underestimated. The reason of this problem is probably because the data used is the indoor model test data, the majority of the anchor plate size is less than 5cm, but the minimum size of the anchor plate collected this time is 0.1m, the maximum is 0.9144m. This shows that the ultimate bearing capacity of the anchor plate has a strong size effect, and the data obtained from small size indoor model test is very unreliable for engineering practice. The three-dimensional unified theoretical solution is similar to PWRC method, which has a similar tendency, but it's more better than that of the latter. the ratio points are evenly distributed on both sides of the 1:1 line and more closer to it.

Statistical analysis of deviation shows that the mean values of Fs are 1.33, 2.687, 1.088, 0.986, and COV of variation coefficients were 0.918, 1.346, 0.582 and 0.351 for the four methods respectively. The accuracy of three-dimentional unified theoretical solution is more than 30% higher than that of PWRC method. Although the mean value is not much different from that of the Terzaghi method, the dispersion degree is also significantly reduced by more than 30%. So the performace of three-dimentional unified theoretical approach is the best.

4 CONCLUSION

In the ultimate pulling state, a quadrature pyramid soil core will be formed before anchor plate. The projection of this soil core onto the vertical plane is a triangle, the shape variation of which can be used to reflect the continuous change regulation of the slip line field before anchor plate with the soil property and buried depth ratio. Based on this, a unified mechanical model was built and limit equilibrium analysis method was used to derive the three-dimensional unified theoretical solution of the ultimate bearing capacity. The rationality of the three-dimensional unified theoretical solution was proved by the comparison with three other theoretical methods and the large size indoor and outdoor test datas.

ACKNOWLEDGEMENTS

The author sincerely acknowledges the financial supports from the national natural science foundation of China (51508141,51878270), research projects of Hunan Provincial Key Laboratory of Geotechnical Engineering for Stability Control and Health Monitoring (E21806) and Hunan university of science and technology (E51857) , which made the present research possible.

REFERENCES

Fukuoka, M., Imamura, Y., Sawada, S., Katada, M., Watanabe,T (1984). Laboratory pullout tests on plate-anchors[C]. Proceedings of the 19th Japanese Geotechnical Society Annual Meeting, Matsuyama, Japan, 1179-1180.

G.S. Kame, D.M. Dewaikar, Deepankar Choudhury (2012). Pullout capacity of a vertical plate anchor embedded in cohesion-less soil[J]. Earth Science Research, 1(1), 27-56.

Karl Terzaghi, Ralph B. Peck, Gholamreza Mesri (1996). Soil mechanics in engineering practice(Third Edition)[M]. New York: John Wiley and Sons, Inc..

Lu Zhaojun, Wu Xiaomin, Zhao Zhaoshen (1983). The experiment research on prototypical anchor-plate's ultimate pullout capacity. Conference proceeding of the 4th soil mechanics and foundation engineering of China Civil Engineering Socity, 164-175.

Miyata, Y., Bathurst, R.J., Konami, T., Dobashi, K (2010). Influence of transient flooding on multi-anchor walls[J]. Soils and Foundations, 50(3), 371-382.

Miyata, Y., Bathurst, R.J., Konami, T. (2011). Evaluation of two anchor plate capacity models for MAW systems[J]. Soils and Foundations, 51(5), 885-895.

Neely, W.J., Stuart, J.G. and Graham, J. (1973). Failure loads of vertical anchor plates in sand[J]. Journal Soil Mechanics and Foundation Division, ASCE, 99(9):669-685.

Public Works Research Center (1995). Technical report on rational design method of reinforced soil walls[R]. Tsukuba, Ibaraki, Japan.

Smith, J.E. (1957). Tests of Concrete Deadman Anchorages in Sand. U.S. Navel Civil Engineering Laboratory (Port Hueneme, California), Technical Memorandum, M-121.

Takeoka, Y., Watanabe, Y., Kodaka, T., Nakano, M. and Noda, T. (2009). Pullout test of reinforcement in sandy soil considering bearing resistance and friction resistance[C]. Proceedings of the 44th Japanese Geotechnical Society Annual Meeting, Yokohama, Japan, 465-466.

Zhang Xuxuan, Wu Xiaomin (1996). A new type of support structure: the theory and practice of anchor-plate soil retaining structure[M]. Beijing: China Railway Publishing House.

Zhu Bi-tang, Yang Min, Guo Wei-dong (2006). Pullout capacity of vertically-burried shallow anchor plates[J]. Chinese Journal of Geotechnical Engineering, 28(10):1236-1241.